Available online at www.sciencedirect.com
SCIENCE DIRECT®

Journal of the European Ceramic Society 23 (2003) 619–627

www.elsevier.com/locate/jeurceramsoc

Long-term stability of nonoxide ceramics in an oxidative environment at 1500 °C

Hagen Klemm[a,*], Christine Taut[b], Gerhard Wötting[c]

[a]*Fraunhofer-Institute for Ceramic Technologies and Sintered Materials, IKTS Dresden, Winterbergstr. 28, D-01277 Dresden, Germany*
[b]*Siemens PG, PS 10 17 55, 45466 Mülheim, Germany*
[c]*H.C. Starck Ceramics GmbH & Co. KG, Lorenz-Hutschenreuther-Str. 81, 95100 Selb, Germany*

Received 4 October 2001; received in revised form 3 July 2002; accepted 14 July 2002

Abstract

In the present study nonoxide ceramic materials based on silicon nitride were evaluated with respect to their long-term oxidation stability at temperatures of 1500 °C. Various Si_3N_4 ceramics with different additive systems were examined after long term oxidation tests (several thousand hours) at 1500 °C in ambient air. Special focus was placed on the processes occurring in the materials during oxidation. In the case of Si_3N_4 materials with sintering additives these processes resulted in alteration of the bulk microstructure which consequently led to degradation of the mechanical properties of the ceramics. The damage mechanisms were discussed on the basis of a comprehensive chemical and microstructural analysis of the materials after the oxidation tests. The diffusion of oxygen into the material and its further reaction in the bulk of the material were found to be the most critical factors during long term oxidation treatment at elevated temperatures. For that reason the long-term bulk stability should be considered as a key requirement for the confident application of potential ceramic materials at temperatures of more than 1400 °C. Finally some possibilities to hinder the processes that occur during long-term service at elevated temperatures are provided.

Keywords: Degradation; Oxidation; Si_3N_4; Strength

1. Introduction

For various industrial and military applications, there is an increasing need for materials that can be used for structural components and that are able to withstand temperatures of 1400 °C and more. For example, for the strategically important field of energy production, an increase in efficiency with a simultaneous decrease in emissions (CO_2, NO_x) necessitates an increase of the gas temperatures in the turbine. Due to environmental requirements, this temperature increase cannot be compensated by additional cooling. For that reason the components in the hot gas path have to be able to withstand higher material temperatures.

The metallic materials presently in use will reach their temperature limit in the foreseeable future. Ceramic materials like silicon nitride are considered to be promising alternative candidates for application at temperatures above 1400 °C due to their superior chemical and physical properties. However, to be successful in such applications, these materials must possess long-term stability under severe thermal/environmental and mechanical loading conditions. Recent development of silicon nitride-based materials is characterized by a remarkable improvement of their mechanical properties (strength, creep and slow crack growth resistance) up to temperatures of 1500 °C, resulting in an improved time-to-failure behavior at elevated temperatures.[1–4] Based on the comprehensive understanding of the damage and failure mechanisms occurring during mechanical loading at elevated temperatures, various benefits were found through the use of new raw materials (powders with improved purity) or the purposeful modification of morphology and chemical composition of grain boundaries in silicon nitride materials. These damage mechanisms are additionally influenced by the interaction of the material with an oxidative environment. The accumulation of damages during these processes will

* Corresponding author. Tel.: +49-351-2553-553; fax: +49-351-2553-600.
E-mail address: klemm@ikts.fhg.de (H. Klemm).

0955-2219/03/$ - see front matter
PII: S0955-2219(02)00267-4

ultimately dictate the performance and lifetime of the material and must be consequently predictable before the structural component can be confidently applied. For that reason a key aim in developing silicon-based nonoxide ceramic materials for long term applications at high temperatures is the comprehensive understanding of these processes, especially focussing on the correlations between microstructural features (e.g. composition and condition of the grain boundary phase) and lifetime determining processes.

Oxidation of silicon nitride materials has been the subject of several scientific studies. Fundamental studies have been performed on pure Si_3N_4 materials (produced by chemical vapor deposition (CVD)) or sintered Si_3N_4 materials with various additive systems.[5–10] Most of these studies described a parabolic oxidation kinetic, suggesting the diffusion of oxygen through the oxidation layer of pure silica as the rate controlling step. Most of these studies deal with tests up to 100 h. In many applications, however, the ceramic components will be subjected to oxidizing conditions at elevated temperatures for thousands of hours. The kinetics of the oxidation process can be calculated from the results of several hours due to the parabolic oxidation mechanism, however, microstructural alternations of the materials were observed as the consequence of diffusion and oxidation processes in the bulk microstructure after long-term oxidation at elevated temperatures.[11–14] In this field the oxidation behavior of the ceramic material cannot be described with oxidation tests up to 100 h. Additionally, significant evidence to the requirement of long-term tests was provided in studies dealing with life time behavior of Si_3N_4 materials at elevated temperatures.[15–17]

In the present study several silicon nitride based ceramic materials were evaluated with respect to their long-term oxidation stability at 1500 °C. As a result of these processes alterations in the bulk and the surface of the materials were observed; this consequently led to degradation of the properties of the ceramics in spite of the optimal combination of properties originally designed during the fabrication. Finally a possibility to hinder the processes that occur during long-term service at elevated temperatures are provided.

2. Experimental

The studies were conducted using Si_3N_4 materials with three additive systems: a HIP'ed Si_3N_4 without sintering additives (HIPSN), and two hot-pressed Si_3N_4 materials with 10 wt.% Y_2O_3 (SNY) and 10 wt.% Y_2O_3, 0.6 wt.% Al_2O_3 (SNYAl) as sintering additives. Si_3N_4–$MoSi_2$ composites were fabricated by the addition of 10 wt.% $MoSi_2$ to the Si_3N_4 material with 10% Y_2O_3 (SNYMo). The materials exhibited microstructures known from the literature to be typical: HIPSN had mainly globular grains with average grain sizes of 0.3 and 2 μm, respectively; and SNY, SNYAl and SNYMo possessed elongated grains with widths between 0.25 and 0.3 μm. The phase composition of the materials was determined by X-ray diffractometry using CuK_α radiation. XRD showed the presence of β-Si_3N_4 with a small amount of α-Si_3N_4 (<5%) and, in the composite, $MoSi_2$. The grain boundary was found to be partially crystalline, with Y-apatite as the crystalline phase, in the Si_3N_4 materials SNY, SNYAl, and SNYMo.

Mechanical testing at ambient and elevated temperatures was carried out in four-point bending geometry with inner and outer spans of 20 and 40 mm, respectively. The oxidation resistance of the materials was studied using bending bars with dimensions of approximately 3 ×4 ×50 mm in a high-temperature furnace at 1500 °C in air with periodical measurement of the weight gain up to 10 000 h.

After the tests, the phase composition of the oxidation surface layer and the bulk region below the oxidation layer was investigated by XRD. To assess the damage caused by the oxidation testing, the bending strengths of the specimens were obtained and compared with the strengths of the as-fabricated samples. Information about the microstructural alterations were obtained by observing polished and plasma-etched (CF_4) cross sections in the SEM.

3. Results and discussion

The results of the oxidation tests on the materials investigated at 1500 °C for 1000 and 2500 h are summarized in Table 1 and illustrated in Fig. 1 as the weight gain as a function of the square root of time. The materials did not obey a pure parabolic oxidation kinetic, reasons of the small deviations are discussed later. Despite of this behavior oxidation rate constants were calculated from the slope of the Δm vs $\sqrt{t}$ plot for

Table 1
Parameters characterizing the oxidation behavior of the materials investigated after 1000 and 2500 h at 1500 °C

	1000 h oxidation		2500 h oxidation			
	Δm (mg/cm^2)	a (μm)	Δm (mg/cm^2)	a (μm)	R (μm^2/h)	K (mg^2/cm^4 s)
HIPSN	0.45	8	0.7	16	0.1	5.2×10^{-8}
SNY	1.7	21	2.2	26	0.3	1.1×10^{-7}
SNYAl	3.57	100	–	–	10	1.1×10^{-6}
SNYMo	2.1	24	2.7	31	0.4	1.2×10^{-7}

a Represents the thickness of the upper oxidation layer measured by SEM, *R* the growth rate of the oxidation layer; *K* parabolic oxidation constant calculated based on the data measured between 1000 and 2500 h or 500 and 1000 h (SNYAl).

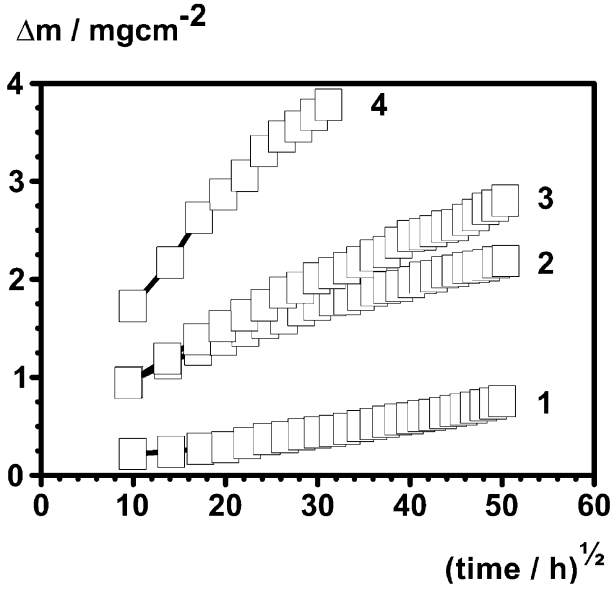

Fig. 1. Oxidation behavior of the materials investigated at 1500 °C, depicted by the weight gain as a function of the square root of time: 1 HIPSN, 2 SNY, 3 SNYMo, 4 SNYAl.

comparison. The oxidation behavior of the materials was found to be strongly dependent on the chemical composition of the oxidation surface layer formed by the oxidation products of the Si_3N_4 and the sintering additives.

The HIP'ed material exhibited the lowest weight gain because a quite clean protective layer of pure SiO_2 with the lowest diffusion coefficient of oxygen [18] was formed. XRD of the oxidation layer showed the presence of crystallized SiO_2 (cristoballite). Only β-Si_3N_4 was detected in the bulk below the oxidation layer. The formation of Si_2ON_2 during the oxidation process was not observed by XRD. The small deviation of the weight gain from a parabolic behavior (slight increase of Δm with the square root of time) should be caused by the formation of cracks during the crystallization of crystoballite, which led consequently to the formation of a interrupted oxidation layer at the surface of the material (higher oxygen diffusion into the material at these areas).

The thickness of the oxidation layer observed in the SEM was found to be about 8 μm after 1000 h and 16 μm after 2500 h oxidation. Fig. 2(A) shows a polished and etched cross section of the HIP'ed Si_3N_4 material after 2500 h of oxidation treatment at 1500 °C. A dense oxidation layer consisting of glassy silica was observed. The cracks found in this oxidation layer are the consequence of the crystallization of cristobalite in combination with volume shrinkage during cooling, as mentioned above. Below the oxidation layer, no differences in the microstructure in comparison to the one in the as-HIP'ed condition were observed. These results are summarized in the schematic diagram in Fig. 2(B).

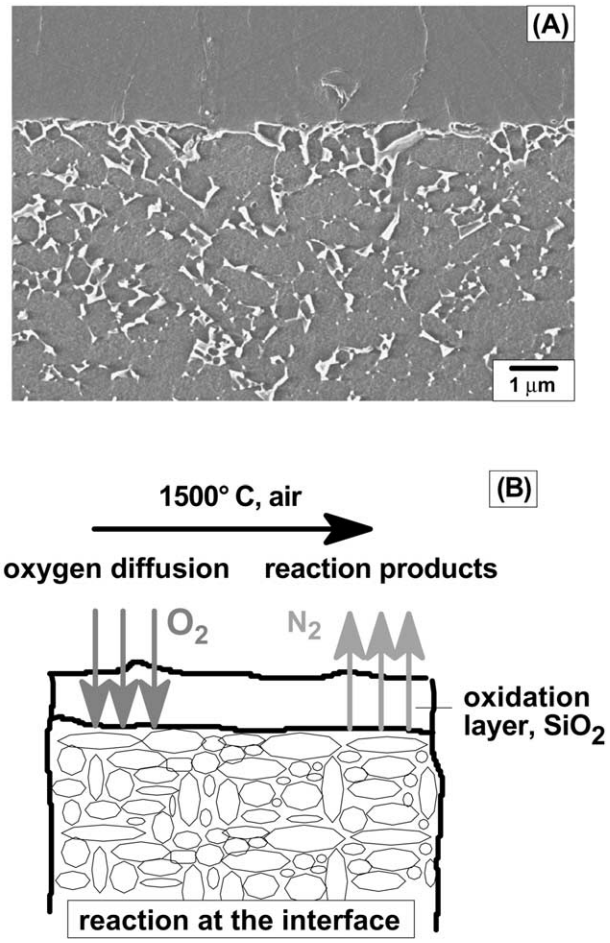

Fig. 2. SEM image of polished and etched cross sections of the HIPed Si_3N_4 material after 2500 h of oxidation treatment at 1500 °C (A), and schematic diagram of the oxidation mechanism of the Si_3N_4 material without sintering additives (B).

All of the oxygen diffusing through the oxidation surface layer reacted at the interface between the SiO_2 layer and the bulk material. The bulk microstructure was not affected by the oxidation process.

In the case of the additive containing materials a significant higher oxidation rate was observed. This behavior, illustrated by comparison of the results obtained in Table 1, was the consequence of increased oxygen diffusion into the material. The upper oxidation layer of these materials consisted of crystalline $Y_2Si_2O_7$ and cristobalite in a glassy layer of SiO_2 containing ions of the sintering additives used (Y^{3+}, Al^{3+}). The presence of these ions of the sintering additives resulted in a change in chemistry and structure of the protective oxidation layer in comparison to the Si_3N_4 without additives. Due to the lower eutectic and viscosity of the oxidation layer, the oxygen diffusion into the material was found to be considerably higher. Some crystalline Si_2ON_2, in addition to Si_3N_4 and $Y_2Si_2O_7$, was detected by XRD in the bulk of the material just beneath the oxidation layer in all sintering additives containing

materials. As shown in Fig. 1 all these materials exhibit a deviation from a pure parabolic behavior, however, in opposite to the Si_3N_4 without additives a slight decrease of the weight gain with the square root of time was observed. The highest deviation from parabolic behavior was found for the material (4) with the lowest oxidation resistance with Y_2O_3/Al_2O_3 as sintering additive.

More information about the oxidation of the SNY and SNY/Al materials was obtained by SEM studies of the surface region of the oxidized specimens. The microstructure of these materials was found to be changed considerably. Fig. 3 shows the microstructure of the SNY/Al material after 1000 h (A, B) and SNY after 2500 h (C, D) oxidation at 1500 °C. In both materials the polished cross section of the surface region exhibited a considerably damaged microstructure with surface damages (C), regions with inhomogeneous distributed grain boundary phase (A, B) and pores extending to the middle of the specimen (C, D), similar to various Si_3N_4 materials described in the literature.[19,20]

In contrast to the additive-free materials, in which the diffusion of the oxygen proceeded only to the interface between the surface oxidation layer and the bulk, some oxygen diffusion into the bulk of the materials with Y_2O_3 and Y_2O_3/Al_2O_3 as sintering additive was observed. This was the consequence of the higher oxygen diffusion in principle and the enlarged dimension of the grain boundaries serving as oxygen diffusion paths in comparison to the additive free material.

A schematic diagram explaining the oxidation mechanism of the sintering additives containing materials is shown in Fig. 4. The oxidation process in these materials occurs predominantly in the glassy phase of (1) the surface oxidation layer and (2) the grain boundaries and triple junctions between the silicon nitride grains in the bulk. It is supposed that the oxidation

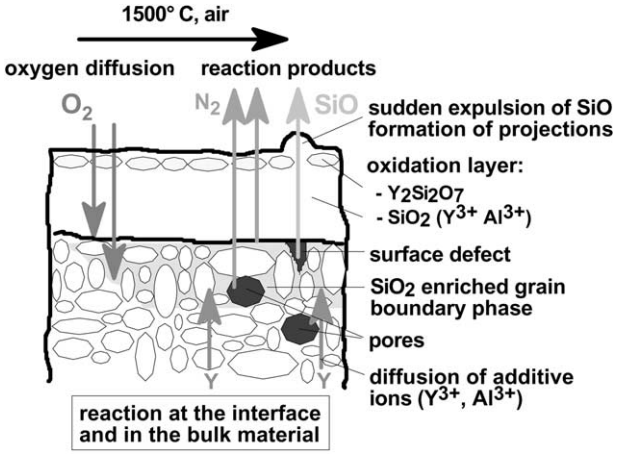

Fig. 4. Schematic diagram of the oxidation mechanism of Si_3N_4 materials with sintering additives.

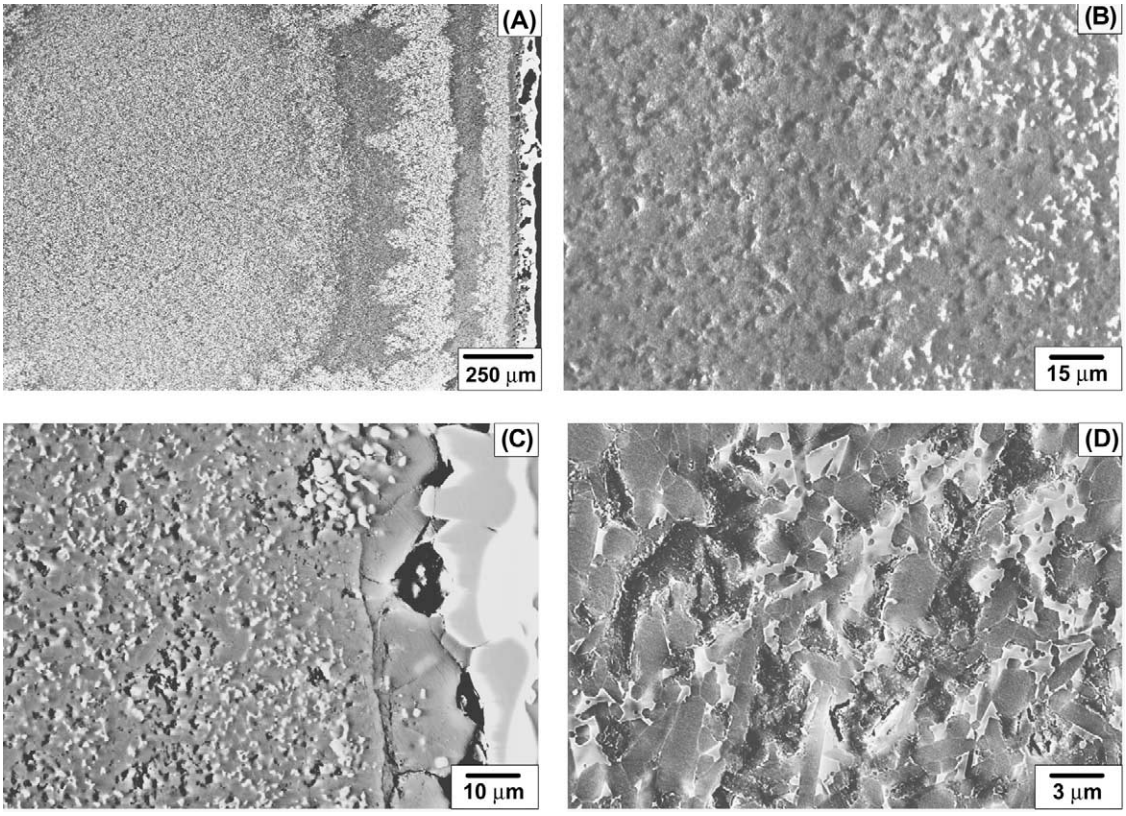

Fig. 3. Microstructural damage in the surface region of the Si_3N_4 materials with Y_2O_3/Al_2O_3, 1000 h (A), (B) and Y_2O_3, 2500 h (C), (D) as sintering additives after oxidation at 1500 °C.

occurring in the upper oxidation scale was controlled by the dissolution of Si_3N_4 into the glassy phase of the oxidation layer. If the rate of the dissolution of Si_3N_4 into the glass was smaller than necessary to react completely with the oxygen diffusing through the upper oxidation layer, the residual oxygen could propagate into the bulk of the Si_3N_4, as observed in the Y_2O_3- and especially in the Y_2O_3/Al_2O_3-containing material used in this study.

This residual oxygen was responsible for the microstructural alterations and damage observed in the additive-containing materials. As a consequence of the reaction of this oxygen in the grain boundaries of the bulk beneath the upper oxidation layer (oxidation of solved Si_3N_4 with formation of SiO_2), an SiO_2 enriched grain boundary phase was formed in this area of the material (see the gray-shaded area in Fig. 4). This SiO_2-rich layer at the surface of the material created a chemical gradient to the composition of the grain boundary phase in the deeper bulk of the Si_3N_4. The relaxation of this chemical gradient was considered to be the reason for the changed microstructure in these Si_3N_4 materials. First, the chemical gradient in the grain boundary phase between the surface and the interior of the bulk material was the driving force for the diffusion of Y^{3+}- and Al^{3+}-ions to the surface of the material, which was presumed to be the main reason for the microstructural alterations observed, e.g. the inhomogeneous distribution of the grain boundary phase.[21]

Evaporation processes were proposed to be a second mechanism occurring during the long-term oxidation test. The oxidation surface of the Si_3N_4 materials exhibited numerous projections which should be the result from bubbles formed as the consequence of sudden gas expulsion [material SNY in Fig. 5(A)]. The SEM image of a fracture surface of the SNY material after 1000 h of oxidation at 1500 °C showed a bubble between the oxidation surface and the bulk material as the fracture origin which has been formed by sudden gas expulsion from the bulk Si_3N_4 material during oxidation [Fig. 5(B)].

In former studies, the oxidation mechanism of Si_3N_4/SiC and $Si_3N_4/MoSi_2$ composite materials was found to be less severe than that of the monolithic Si_3N_4 materials, with the consequence of an improved microstructural and mechanical stability after high-temperature oxidation.[9,19,20,22] These results were attributed to the microstructural development of the composite materials during the oxidation treatment, namely a significantly lower degree of damage than that in the Si_3N_4 materials reported above, although the oxidation processes also occurred in the bulk of the composites. The numerous projections observed at the oxidation surface of the materials SNYAl and SNY [Fig. 5(A) and (B)] were not found at the oxidation surface of the Si_3N_4–$MoSi_2$ composite. As shown in Fig. 6, no surface damages, pores or inhomogenities of the grain boundary phase were found in the oxidized $Si_3N_4/MoSi_2$ composite specimen. The changed oxidation mechanism in comparison to the Si_3N_4 material is demonstrated in the schematic diagram in Fig. 7(A). Similar to the Si_3N_4 material a part of the oxygen penetrated through the grain boundaries and triple junctions into the upper region of the bulk material and reacted with the Si_3N_4 present in the oxinitride glass.

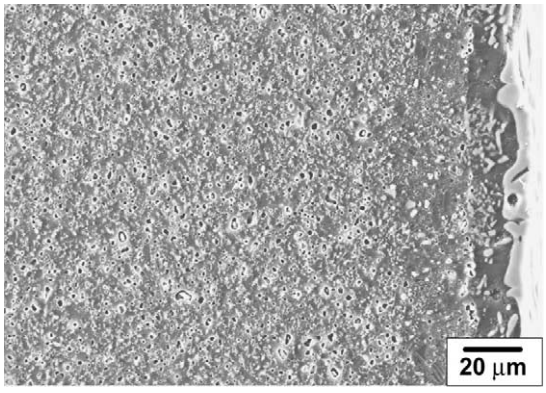

Fig. 6. SEM image of polished cross sections of the Si_3N_4–$MoSi_2$ composite after 2500 h of oxidation treatment in air at 1500 °C.

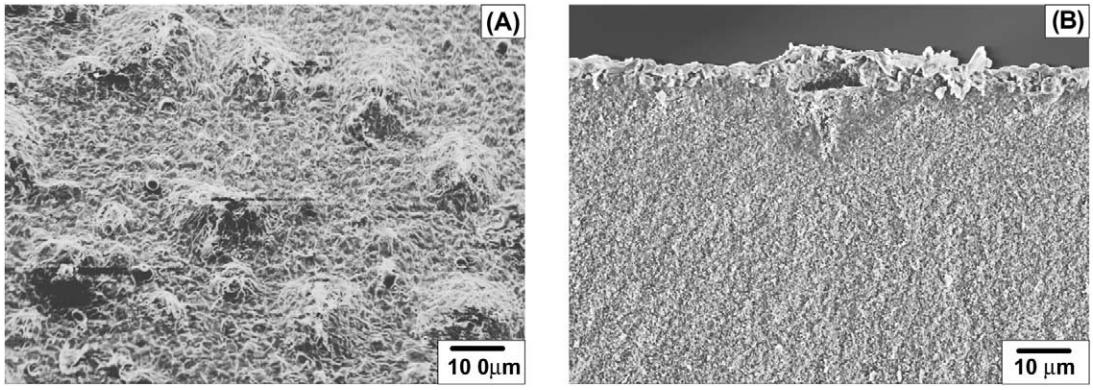

Fig. 5. Bubble formation as the consequence of evaporation processes at the oxidation surface (A) and the fracture surface (B) of the silicon nitride SNY.

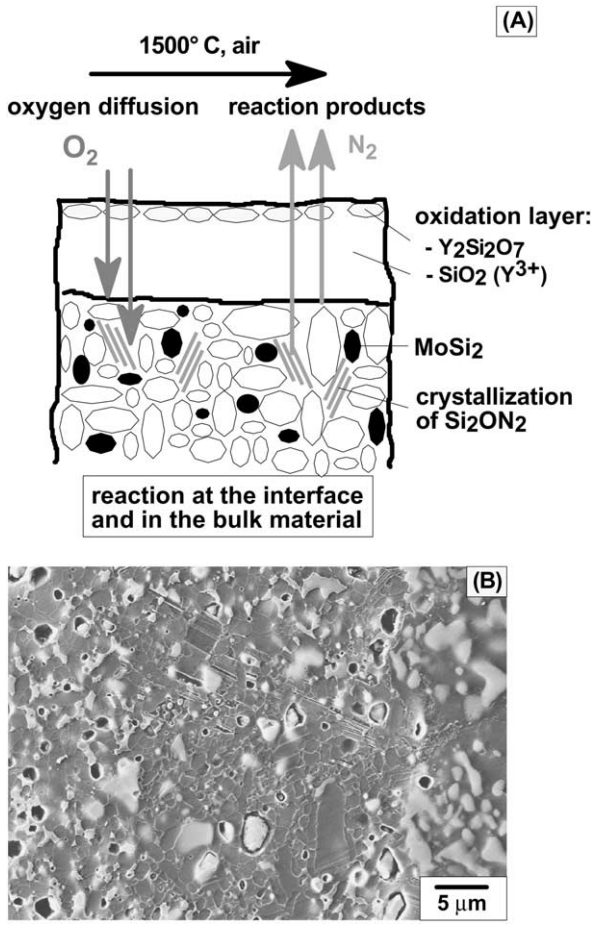

Fig. 7. Schematic diagram of the oxidation mechanism of the Si_3N_4–$MoSi_2$ composite (A) and Si_2ON_2 interlayer in the upper bulk (B) of the Si_3N_4–$MoSi_2$ composite material after 2500 h oxidation at 1500 °C in air.

However, instead of the SiO_2 in the Si_3N_4 material, crystalline Si_2ON_2 was found to be the main oxidation product in the composite material.

Si_2ON_2 has already been found as an oxidation layer at the Si_3N_4/SiO_2 interface for CVD Si_3N_4 in former studies.[23–26] In the HIPed Si_3N_4 material of this study, however, any formation of a Si_2ON_2 interface layer was not observed. The reasons for this behavior are presumed to be different test conditions with a higher temperature and exposure time in comparison to the of the data in literature.[27] Furthermore the oxidation mechanism was found to be changed as the consequence of the presence of the yttria or alumina as sintering additive in the material of this study. In the case of the CVD materials or the HIPed Si_3N_4 without additives the oxidation took place only at the interface between the oxidation layer and the bulk material. As the consequence of additional oxygen diffusion into the bulk of Si_3N_4 materials with sintering additives oxidation processes took place in the grain boundaries and triple junctions of the material. The typical appearance of the Si_2ON_2 with partial-fiber, twin-like grains [as shown in the SEM image of a polished and plasma-etched section in Fig. 7(B)] located in the bulk material show that they are not the consequence of the oxidation processes at the interface but the result of the oxidation and crystallization processes in the grain boundary phase in the bulk of the material. The $MoSi_2$ in this region was partially oxidized with the formation of Mo_5Si_3 as proposed for the oxidation of $MoSi_2$ in lower oxygen partial pressures.[28]

$$5\ MoSi_2 + 7O_2 \rightarrow Mo_5Si_3 + 7\ SiO_2 \quad (1)$$

It is supposed, that with this reaction the crystallization of Si_2ON_2 was stimulated by an increased formation of crystallization nuclei.

The formation of an SiO_2-rich grain boundary phase in the upper region of the bulk was prevented; thus, there was no driving force for diffusion and evaporation processes and no subsequent change in the microstructure of the material. The damage processes described for the monolithic Si_3N_4 did not occur even after an application-relevant, long-term oxidation treatment of 10 000 h at 1500 °C, as shown in Fig. 8.

The comparison of the oxidation behavior of the Si_3N_4 materials studied provides additional evidence for the evaporation processes in the additive containing Si_3N_4 materials as described above. In opposite to the additive free Si_3N_4, a decreased weight gain rate with the square root of time (Fig. 1) was observed only in the sintering additives containing materials where oxidation processes took place in the upper region of the bulk too. Comparing the materials SNY (2) and SNYMo (3) a higher weight gain with a oxidation kinetic more near to a parabolic behavior was observed for the composite with $MoSi_2$. This result couldn't be expected from chemical point of view. Both materials formed a similar oxidation surface layer with similar oxygen permeability due to the use of the same sintering additive system. Furthermore, caused by the evaporation of MoO_3, oxidation product of $MoSi_2$, the weight gain of the composite should be rather smaller in comparison to the SNY material.

The different behavior should be explained with the oxidation reactions in the grain boundaries of the upper region of the bulk material which led consequently to the formation of the projections by outgassing observed only at the oxidation surface of the materials SNYAl and SNY [Fig. 5(A) and (B)] without $MoSi_2$ addition. The formation of a smaller amount of N_2 in the case of the composites seems to be one possibility for the formation of these projections at the oxidation surface; however, during the oxidation to all products, SiO_2 and Si_2ON_2, the same quantity of N_2 is formed from the reaction of the Si_3N_4 with a defined amount of oxygen diffusing into the materials:

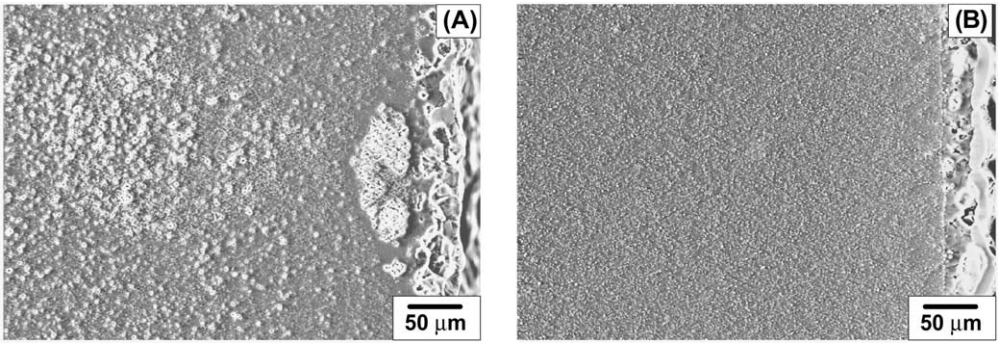

Fig. 8. Comparison of the surface region of a polished cross section of the monolithic Si_3N_4 SNY (A) and the Si_3N_4–$MoSi_2$ composite SN Mo (B) after 10 000 h of oxidation at 1500 °C in air.

$$3\ O_2 + Si_3N_4 \rightarrow 3\ SiO_2 + 2\ N_2 \quad (2)$$

$$3\ O_2 + 4\ Si_3N_4 \rightarrow 6\ Si_2ON_2 + 2\ N_2 \quad (3)$$

An other gas in the system is SiO, which should not be formed in significant quantities under these conditions, i.e. a high oxygen partial pressure. However, with the formation of a SiO_2 enriched grain boundary phase as the consequence of the oxidation processes in the bulk a supersaturation of SiO_2 in the glassy phase just beneath the oxidation layer seems to be possible. The lower oxygen partial pressure in the grain boundaries and triple junctions in this region of the Si_3N_4 material should allow a local relaxation of this SiO_2 rich grain boundary phase with the formation and sudden expulsion of SiO from the bulk, resulting in the formation of the projections from gas bubbles trapped in the oxidation layer (Fig. 5). An additional argumentation to these processes was given in a previous report[22] comparing a Si_3N_4 materials with Si_3N_4–$MoSi_2$ and Si_3N_4–SiC composites after long-term oxidation tests.

Besides the stability of the upper surface scale, which was found to be a critical factor especially in wet environments,[29–32] the stability of the microstructure is an essential requirement for successful long-term application of ceramic materials at elevated temperatures. The microstructure originating from the processing and sintering of the ceramic material is the main factor determining the properties of a ceramic part. Any changes in the microstructure of a ceramic material during long-term service at elevated temperatures, such as those observed in the Si_3N_4 material, will cause property degradation. This behavior can be demonstrated using the residual flexural strength of the materials, measured after different times up to 10 000 h oxidation at 1500 °C and compared with that after hot pressing (Fig. 9). Due to the severe microstructural damages observed in the Si_3N_4 material, a significant degradation in strength was measured, with a value of about 260 MPa after 10 000 h (32% of the hot pressed condition). After the same oxidation time the composite material exhibited a residual strength of more than 500 MPa (65% of the hot pressed condition). The fracture origins of all specimens tested were found to be defects caused by oxidation damage at the surface of the materials.

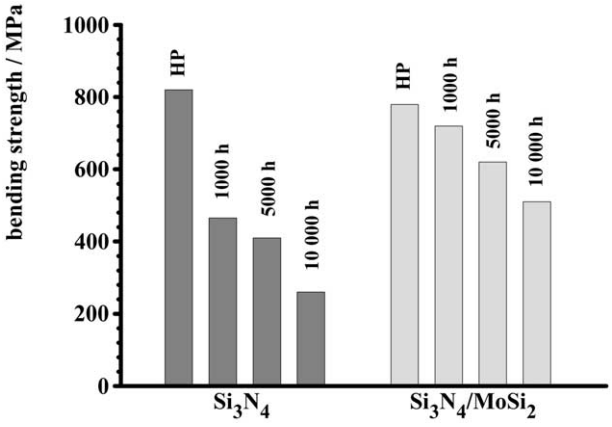

Fig. 9. Comparison of the bending strength of the Si_3N_4 material SNY and the Si_3N_4–$MoSi_2$ composite as hot pressed and after several times of oxidation treatment at 1500 °C.

4. Conclusions

The main factor influencing the long term oxidation of the non-oxide ceramic materials is diffusion of oxygen through the protective surface layer formed during oxidation at elevated temperatures. An oxidation protection layer with minimal diffusion coefficient of oxygen was found to be strongly desirable, especially in long-term applications at elevated temperatures. This can be achieved in silicon-based materials by the formation of a nearly pure layer of SiO_2 featured by the lowest oxygen permeability in comparison to other oxide materials. Any addition of other ions, e.g. cations from the sintering aids, lead to an increase of the oxygen diffusion into the material caused by a lower eutectic and viscosity of the silicate glass formed in comparison to a pure silica layer.

However, diffusion of a small amount oxygen into the ceramic material will occur and cannot be prevented

completely. The question, where and how does the diffusion oxygen react in the material, should be considered as the second important problem in the development of oxidation stable non-oxide ceramic materials. The complete reaction of the diffusion oxygen at the interface between the oxidation layer and the bulk without affecting the bulk microstructure was found to be the optimal mode. In many cases, however, a part of the oxygen diffused into the microstructure of the bulk material. The reaction of this oxygen was found to be the main reason for microstructural alternations which led consequently to degradation of the mechanical properties of the materials. With the Si_3N_4–$MoSi_2$ composite an example for an effective method to overcome the problems from the inner oxidation processes was demonstrated. The microstructure of the silicon nitride material could be stabilized by a defined reaction of the diffusion oxygen to a less reactive oxidation product. In general, as the consequence of the microstructural damage demonstrated with the example of the Si_3N_4 materials, an accurate control of all processes occurring in the microstructure, especially during long-term service at elevated temperatures in oxidative environment, is strongly recommended in the development of high-temperature stable ceramic materials.

References

1. Menon, M. N., Fang, H. T., Wu, D. C., Jenkins, M. G., Ferber, M. F., More, K. L., Hubbard, C. R. and Nolan, T. A., Creep and stress rupture behavior of an advanced silicon nitride, Part I—III. *J. Am. Ceram. Soc.*, 1994, **77**(5), 1217–1241.
2. Rendtel, A., Hübner, H., Herrmann, M. and Schubert, Ch., Si_3N_4/SiC nanocomposite materials: II. Hot strength, creep, and oxidation resistance. *J. Am. Ceram. Soc.*, 1998, **81**(5), 1109–1120.
3. Lofaj, F., Cao, J. W., Okada, A. and Kawamoto, H., Comparison of creep behavior and creep damage mechanisms in the high-pereformance silicon nitrides. In *Proc. 6th Int. Symp. Ceram. Mater. & Engines*, ed. K. Niihara, S. Hirano, S. Kanzaki, K. Komeya, K. Morinaga. Technoplaza Co., Ltd., 1997, pp. 576–581.
4. Lofaj, F., Wiederhorn, S., Long, G., Jemian, P. and Ferber, M., Cavitation creep in the next generation silicon nitride. In *Proc. 7th Int. Symp. Ceram. Mater. & Engines*, ed. J. Heinrich and F. Aldinger. Wiley, VCH, 2000, pp. 487–493.
5. Hirai, T., Niihara, K. and Goto, T., Oxidation of CVD Si_3N_4 at 1550°C to 1650 °C. *J. Am. Ceram. Soc.*, 1980, **63**(7–8), 1550 419–424.
6. Opila, E. J., Fox, D. S. and Barrett, C. A., Cyclic oxidation of monolithic SiC and Si_3N_4 Materials. *Ceram. Eng. Sci. Proc*, 1973, **14**(7–8), 367–374.
7. Fox, D. S., Oxidation behavior of chemically-vapor-deposited silicon carbide and silicon nitride from to 1600 °C. *J. Am. Ceram. Soc.*, 1200, **81**(4), 1998 945–950.
8. Ogbuji, L. U. and Opila, E. J., A comparison of the oxidation kinetics of SiC and Si_3N_4. *J. Electrochem. Soc.*, 1995, **142**(3), 925–930.
9. Klemm, H., Herrmann, M. and Schubert, Chr., High temperature oxidation and corrosion of silicon-based nonoxide ceramics. In *ASME Turbo Expo '98*, Stockholm, Sweden 1998, ASME Paper 98-GT-480.
10. Nickel, K. G., Fu, Z. and Quirmbach, P., High temperature oxidation and corrosion of engineering ceramics. *Trans. ASME*, 1993, **76**(115), 76–82.
11. Tressler, R. E., Environmental effects on long term reliability of SiC and Si_3N_4-ceramics. In *Ceram. Trans.*, Vol. 10, ed. R. E. Tressler, 1990, pp. 99–124.
12. Jacobson, N. S., Corrosion of silicon-based ceramics in combustion environments. *J.Am. Ceram. Soc.*, 1993, **76**(1), 3–28.
13. Van der Biest, O., Weber, C. and Garguet, L. A., Role of oxidation on creep and high-temperature failure of silicon nitride. In *Proc. 3th Int. Symp. Ceram. Mater. & Components for Engines*, ed. V. Tennery, Columbus, OH, 1989, pp. 729–738.
14. Nishimura, N., Masuo, E. and Takita, K., Effect of microstructural degradation on the strength of silicon nitride after high-temperature exposure. In *Proc. 4th Int. Symp. Ceram. Mater. & Components for Engines*, ed. R. Carlson, T. Johansson and T. Kahlman. Elsevier, London, 1991, pp. 1139–1149.
15. Wereszczak, A. A., Ferber, M. K., Kirkland, T. P., More, K. L., Foley, M. R. and Yeckley, R. L., Evolution of stress failure resulting from high-temperature stress-corrosion cracking in a hot isostatically pressed silicon nitride. *J. Am. Ceram. Soc.*, 1995, **78**(8), 2129–2140.
16. Wereszczak, A. A., Breder, K. and Ferber, M. K., Role of oxidaton in the time-dependent failure behavior of hot isostatically pressed silicon nitride at 1370°C. *J. Am. Ceram. Soc.*, 1993, **76**(11), 2919–2922.
17. Rendtel, P., Rendtel, A., Hübner, H., Klemm, H. and Herrmann, M., Effect of long-term oxidation on creep and failure of Si_3N_4 and Si_3N_4/SiC nanocomposites. *J. Eur. Ceram. Soc.*, 1999, **19**(2), 217–226.
18. Courtright, E. L., Engineering property limitations of structural ceramics and ceramic composites above 1600°C. *Ceram. Eng. Sci. Proc*, 1600, **12**(9–10), 1991 1725–1744.
19. Klemm, H., Tangermann, K., Schubert, Chr. and Hermel, W., Influence of molybdenum silicide additions on high-temperature oxidation resistance of silicon nitride materials. *J. Am. Ceram. Soc.*, 1996, **79**(9), 2429–2435.
20. Klemm, H., Herrmann, M. and Schubert, Chr., High temperature oxidation of silicon nitride based ceramic materials. In *Proc. 6th Internat. Symp. on Ceram. Mater. & Comp. for Engines*, Arita, Japan, 1997, pp. 576–581.
21. Clarke, D. R., Thermodynamic mechanism for cation diffusion through an intergranular phase: application to environmental reactions with nitrogen ceramics. In *Progress in Nitrogen Ceramics, NATO ASI Series, Series E: Applied Sciences, No. 65*, ed. F. L. Riley. Martinus Nijhoff, The Hague, The Netherlands, 1983, pp. 421–426.
22. Klemm, H., Herrmann, M. and Schubert, Chr., Silicon nitride materials with an improved high temperature oxidation resistance. *Ceram. Eng. & Sci. Proc.*, 1997, **18**(3), 615–623.
23. Du, H., Dressler, R. E., Spear, K. E. and Pantano, C. G., Oxidation studies of crystalline CVD silicon nitride. *J. Electrochem. Soc.*, 1989, **136**(5), 1527–1536.
24. Ogbuji, L. U. and Smialek, J. L., TEM evidience for oxinitride layer in the oxidation of Si_3N_4. *J. Electrochem. Soc.*, 1991, **138**(10), L51–L53.
25. Ogbuji, L. U., Role of Si_2ON_2 in the passive oxidation of chemically-vapor-deposited Si_3N_4. *J. Am. Ceram. Soc.*, 1992, **75**(11), 2995–3000.
26. Ogbuji, L. U. and Bryan, S., The SiO_2/Si_3N_4 interface, part I: nature of the interface. *J. Am. Ceram. Soc.*, 1995, **78**(5), 1272–1284.
27. Ogbuji, L., Private communication, 2000.
28. Zhu, Y. T., Stan, M., Conzone, S. D. and Butt, D. P., Thermal oxidation kinetics of $MoSi_2$-based powders. *J. Am. Ceram. Soc.*, 1999, **82**(10), 2785–2790.
29. Robinson, R. C. and Smialek, J. L., SiC recession caused by SiO_2

scale volatility under combustion conditions: I, experimental results and empirical model. *J. Am. Ceram. Soc.*, 1999, **82**(7), 1817–1825.

30. Opila, E. J., Smialek, J. L., Robinson, R. C., Fox, D. S. and Jacobson, N. S., SiC recession caused by SiO_2 scale volatility under combustion conditions: II, thermodynamics and gaseous-diffusion model. *J. Am. Ceram. Soc.*, 1999, **82**(7), 1826–1834.
31. Filsinger, D., Schulz, A., Wittig, S., Taut, C., Klemm, H. and Wötting, G., Model combustor to assess the oxidation behavior of ceramic materials under real engine conditions. In *ASME Turbo Expo '99*, Indianapolis, USA, 1999, ASME Paper 99-GT-349.
32. Klemm, H., Schubert, Chr., Taut, Chr., Schulz, A. and Wötting, G., Corrosion of non-oxide silicon-based ceramics in a gas turbine environment. In *Proc. 7th Symp. Ceram Mater. & Comp. for Engines*. Wiley-VCH Verlag, Weinheim, 2000, pp. 153–156.